

Electrostatics and electrical transport in semiconductor nanowire Schottky diodes

Cheng-Han Hsu, Qiaoming Wang, Xin Tao, and Yi Gu

Citation: *Appl. Phys. Lett.* **101**, 183103 (2012); doi: 10.1063/1.4765653

View online: <http://dx.doi.org/10.1063/1.4765653>

View Table of Contents: <http://apl.aip.org/resource/1/APPLAB/v101/i18>

Published by the [American Institute of Physics](http://www.aip.org).

Related Articles

Polycrystalline ZnO Mott-barrier diodes

Appl. Phys. Lett. **101**, 173509 (2012)

Thermally driven unipolar and bipolar spin diode based on double quantum dots

J. Appl. Phys. **112**, 084324 (2012)

Temperature-dependent properties of semimetal graphite-ZnO Schottky diodes

Appl. Phys. Lett. **101**, 162106 (2012)

Millimeterwave Schottky diode on graphene monolayer via asymmetric metal contacts

J. Appl. Phys. **112**, 084302 (2012)

Electrical and microstructural analyses of 200MeV Ag¹⁴⁺ ion irradiated Ni/GaN Schottky barrier diode

Appl. Phys. Lett. **101**, 153508 (2012)

Additional information on *Appl. Phys. Lett.*

Journal Homepage: <http://apl.aip.org/>

Journal Information: http://apl.aip.org/about/about_the_journal

Top downloads: http://apl.aip.org/features/most_downloaded

Information for Authors: <http://apl.aip.org/authors>

ADVERTISEMENT

Universal charged-particle detector
for interdisciplinary applications:

- Non-scanning Mass Spectrometry
- Non-scanning Ion Mobility Spectrometry
- Non-scanning Electron Spectroscopy
- Direct microchannel plate readout
- Thermal ion motion and mobility studies
- Bio-molecular ion soft-landing profiling
- Real-time beam current/shape tuning
- Diagnostics tool for instrument design
- Compact linear array for beam lines

Contact OI Analytical: +1-205-733-6900



Electrostatics and electrical transport in semiconductor nanowire Schottky diodes

Cheng-Han Hsu, Qiaoming Wang, Xin Tao, and Yi Gu^{a)}

Department of Physics and Astronomy, Washington State University, Pullman, Washington 99164, USA

(Received 23 August 2012; accepted 17 October 2012; published online 29 October 2012)

The electrostatics and electrical transport characteristics in semiconductor nanowire Schottky diodes are studied using three-dimensional finite-element simulations. From the simulations, the dependences of the depletion region width on the bias and the doping level are found to deviate significantly from the relations in the bulk Schottky model, indicating different electrostatic properties in nanowire Schottky junctions. Furthermore, simulations of the current-voltage relation, which is corroborated by experimental measurements, demonstrate that the standard analytical model is not sufficient to describe current-voltage characteristics in nanowire Schottky diodes. An important implication is that the commonly used analytical model is not valid for extracting the ideality factor and the Schottky barrier height. These findings suggest that numerical simulations are critical to evaluating nanoscale device performance and guiding device development efforts.

© 2012 American Institute of Physics. [<http://dx.doi.org/10.1063/1.4765653>]

Metal-semiconductor contacts are a critical component in electronics. The electrical properties of these contacts, especially those of Schottky contacts, play an important role in determining device performance. The model of Schottky contacts in bulk devices is well established. However, studies have shown that the bulk model is inadequate to describe the behaviors of Schottky junctions in semiconductor nanostructures,^{1–3} in particular semiconductor nanowires, due to the reduced material dimension and different contact geometries. As an example, an exponential dependence of the depletion region width on the applied bias, as opposed to the square-root dependence in the bulk model, was suggested by simulations of “end-on” Ge nanowire Schottky contacts.³ On the other hand, a linear dependence was experimentally observed in “side-on” ZnO nanowire Schottky junctions.⁴ A better understanding of the electrostatics and electrical transport is critical to device applications, including nanowire-based metal-semiconductor-metal photodetectors^{5,6} and Schottky-barrier field-effect transistors.⁷ Studies of fundamental material properties in the nanoscale, such as probing carrier and exciton transport facilitated by the Schottky contact as the carrier collector,^{4,8,9} will also benefit greatly from a detailed knowledge of nanoscale Schottky junction characteristics.

In this work, we use three-dimensional (3D) finite-element simulations to gain insight into the electrostatics and electrical transport in Schottky junctions in semiconductor nanowires, particularly ZnO nanowires. Experimental results are also presented to corroborate the simulations, particularly the current-voltage relations. The simulations are based on solving Poisson’s equation and carrier continuity equations in a self-consistent manner, and take into account Schottky barrier lowering due to the image force and carrier velocity saturation under high electric fields. We focus on the “side-on” contact geometry, which is one of the most common configurations and easiest to fabricate. Simulations of the

“end-on” geometry have been reported in a previous study.¹⁰ Our results show that the depletion region width as a function of the bias depends on the doping level: it is linear (sub-linear) with high (low) doping levels. Furthermore, via the simulations of the current-voltage relations, we suggest that the common procedures based on standard analytical model are not suitable for extracting the ideality factor and the Schottky barrier height in nanowire Schottky diodes. These findings provide insight into the characteristics of Schottky junctions in semiconductor nanowires, and facilitate Schottky-based nanoscale device development.

Details of the ZnO nanowire growth and fabrications of single nanowire Schottky diodes can be found in Refs. 8 and 11. Briefly, Pt and Ti/Au were used as the Schottky and ohmic side-on electrodes, respectively. Heavily doped Si wafers coated with a 200 nm Si₃N₄ layer were used as the device substrates. 3D schematic device geometry with side-on contacts and a scanning electron microscopy (SEM) image of a device are shown in Fig. 1(a) and the inset to Fig. 1(b), respectively. The rectifying current-voltage (I-V) relation measured from a typical device, shown in Fig. 1(b), is consistent with the Schottky (ohmic) nature of the Pt (Ti/Au) contacts. The device configuration shown in Fig. 1(a) is used in the finite-element simulations, where the 3D Poisson’s equation,

$$\nabla^2 \phi = -\frac{q}{\epsilon}(p - n + N_D^+) \quad (1)$$

and the charge carrier continuity equations

$$\frac{1}{q} \vec{\nabla} \cdot [q\mu_n(\epsilon)n\vec{E} + qD_n(\epsilon)\vec{\nabla}n] = \frac{1}{q} \vec{\nabla} \cdot (q\mu_p p\vec{E} + qD_p \vec{\nabla}p) = 0, \quad (2)$$

were solved in a self-consistent manner. Materials parameters used in the simulations are listed in Table I. The electron and hole diffusivities, D_n and D_p , are calculated as $(kT/q)\mu_n$

^{a)} Author to whom correspondence should be addressed. Electronic mail: yigu@wsu.edu.

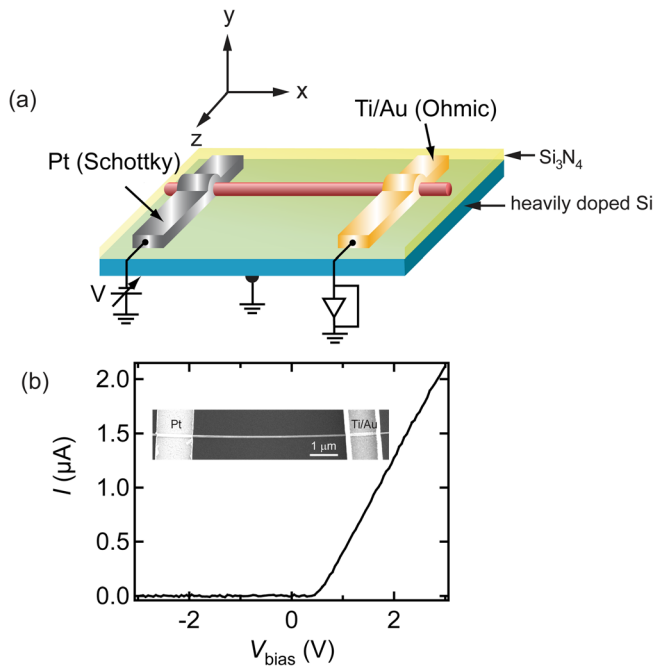


FIG. 1. (a) Schematic device configuration; (b) current-voltage relation of a ZnO nanowire Schottky diode with the inset showing a SEM image of a nanowire Schottky diode.

and $(kT/q)\mu_p$, respectively. As the as-grown ZnO nanowires are n-type doped,⁸ shallow donors with an activation energy of 46 meV were defined in the simulation. This activation energy corresponds to hydrogen donors,^{12,13} the dominant shallow donor species in as-grown ZnO, and this value is

TABLE I. ZnO parameters used in the simulation.

Bandgap	Dielectric constant (ϵ)	Electron (hole) effective mass	Electron mobility	Hole mobility	Barrier height of Pt/ZnO
3.33 eV	8.66	0.24 (0.8) m_0	See supplemental information		0.75 V

verified by variable-temperature electrical measurements of ZnO nanowires.¹⁴ The charge carrier densities were calculated using Fermi-Dirac statistics.

The electrical current in the nanowire Schottky diodes was calculated using the drift-diffusion model, with the boundary condition at the Schottky contact described by the thermionic emission theory.^{15,16} The image-force-induced Schottky barrier lowering, which is given by $\sqrt{\frac{q|\vec{E} \cdot \hat{n}|}{4\pi\epsilon}}$, with \hat{n} as the normal vector pointing from the semiconductor region to the metal contact, was included in the model. To account for the electron drift velocity saturation under high fields, i.e., μ_n as a function of ϵ , the mobility model by Canali *et al.*,¹⁷ was used. Parameters of this model were obtained by fitting the electron drift velocity vs. electric field in ZnO calculated by Monte-Carlo methods.¹⁸ We note that the tunneling effect was not included here, since the reverse-biased current is very small (~ 10 – 100 pA, which is the noise floor of our electrical measurement circuit) in our nanowire devices, indicating negligible tunneling current. As such, the ideal Schottky junction was considered here in the simulations.

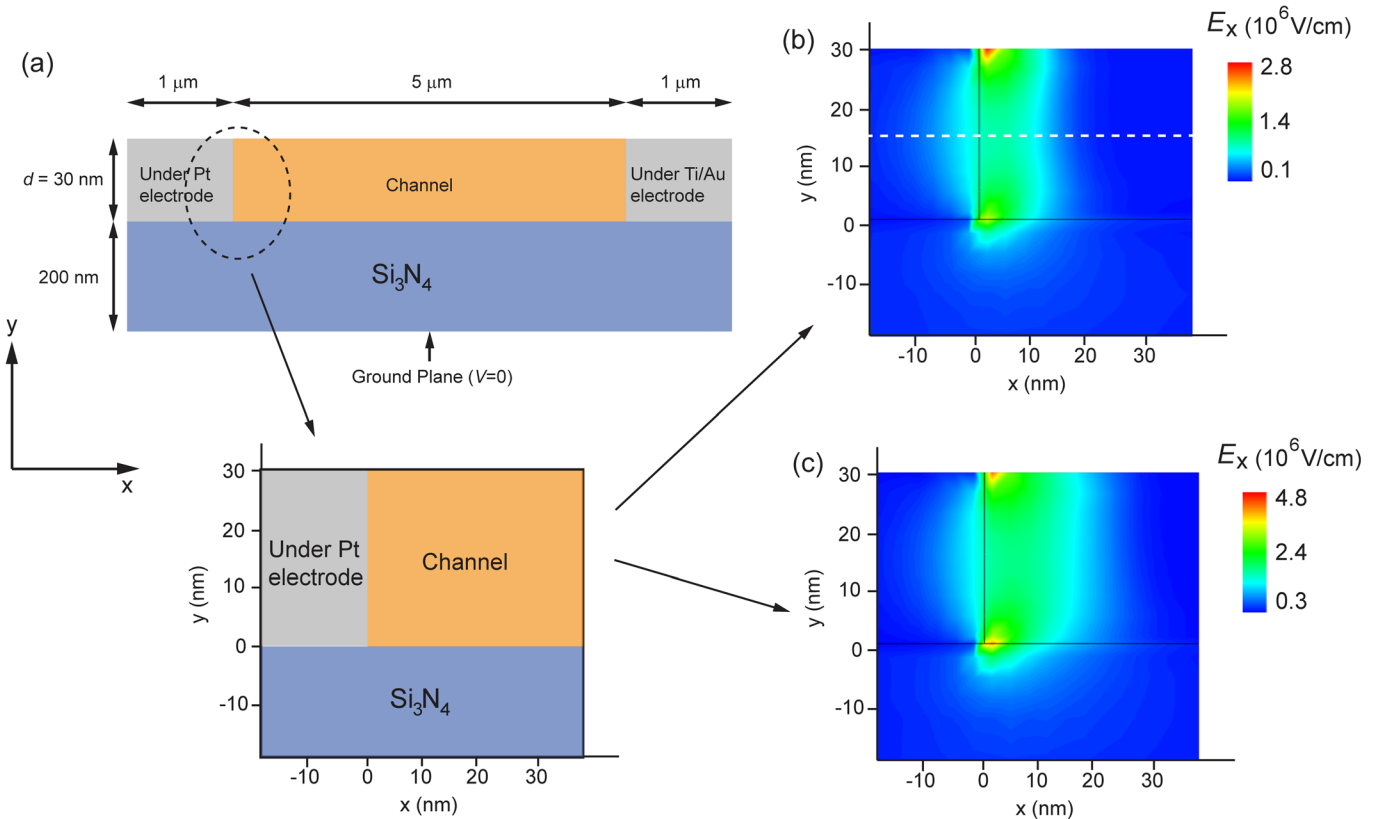


FIG. 2. (a) Cross-section (x - y plane) view of the device geometry for a 30 nm diameter ZnO nanowire, with the lower panel showing the configuration of the plots in (b) and (c); the x component of the simulated electric field at a bias of (b) -3 V and (c) -5 V, for an N_D of $5 \times 10^{18} \text{ cm}^{-3}$. The dashed line in (b) indicates the location where the line profile was obtained (Fig. 3).

We first consider the electrostatics of the nanowire Schottky junctions, particularly the depletion region width under the reverse-biased condition. In this case, the Schottky contact was negatively biased, and the ohmic contact was grounded in the simulations. Figure 2(a) shows a cross-section view of a ZnO nanowire Schottky diode with a diameter of 30 nm in the x - y plane [the 3D orientation scheme is shown in Fig. 1(a)]. The total length of the nanowire is 7 μm , and each electrode (Schottky and ohmic) has a width of 1 μm ; this corresponds to the real dimensions of our fabricated devices. The electrical contacts were defined on the periphery of the nanowire, corresponding to the side-on configuration. The heavily doped Si substrate underneath the 200 nm Si_3N_4 layer [see also Fig. 1(a)] was treated as a metal, which was connected to the ground. The simulated electric fields along the x direction, i.e., E_x , for a donor concentration (N_D) of $5 \times 10^{18} \text{ cm}^{-3}$, with the Schottky electrode biased at -3 V and -5 V , are shown in Figs. 2(b) and 2(c), respectively. It is clear that higher negative biases lead to a larger depletion region, indicated by the extension of E_x into the channel region. For measuring the depletion region width (W_{dep}), the line profiles of E_x at the center of the nanowire, with an example shown by the dashed line in Fig. 2(b), were plotted in Fig. 3(a). W_{dep} was defined as the distance between the edge of the electrode ($x=0$), and the point at which E_x becomes zero.

W_{dep} as a function of bias was obtained for different N_D , and results are shown in Fig. 3(b). For N_D of 10^{19} cm^{-3} ,

W_{dep} is almost linearly dependent on the bias, different from the square-root dependence in bulk Schottky junctions, which is given by $\sqrt{\frac{2\epsilon}{qN_D}(V_{\text{bi}} - V_{\text{bias}} - \frac{kT}{q})}$, with V_{bi} as the built-in potential. A linear dependence has been experimentally observed in ZnO nanowires with side-on Schottky contacts⁴ and also in crossed CdS/Si nanowire Schottky junctions.¹⁹ This deviation from the standard Schottky model was attributed to the small dimensions of the Schottky junctions.^{4,19} In addition, surface effects were also suggested as an important origin.⁴ Our results indicate that such a linear behavior is an intrinsic property of nanowire Schottky junctions, since no surface/interface states were considered in the simulations. Furthermore, as N_D decreases, our simulations show that the dependence of W_{dep} on the bias becomes more sublinear but is still different from the square-root relation [Figs. 3(c)–3(e)]. In all cases, W_{dep} is significantly higher than the value calculated from the bulk Schottky model. Besides the unusual bias dependence, W_{dep} as a function of N_D also deviates from the bulk behavior: as shown in Fig. 3(f), instead of following the square-root relation with $N_D^{-1/2}$ (dashed line), W_{dep} exhibits an exponential relation. Previous calculations²⁰ of metal-carbon-nanotube contacts have revealed a similar exponential dependence. These findings suggest that the electrostatics in nanowire Schottky junctions is different from that described by the standard bulk model.

Following this, an important issue is the impact of the different electrostatics on the electrical properties of nanowire

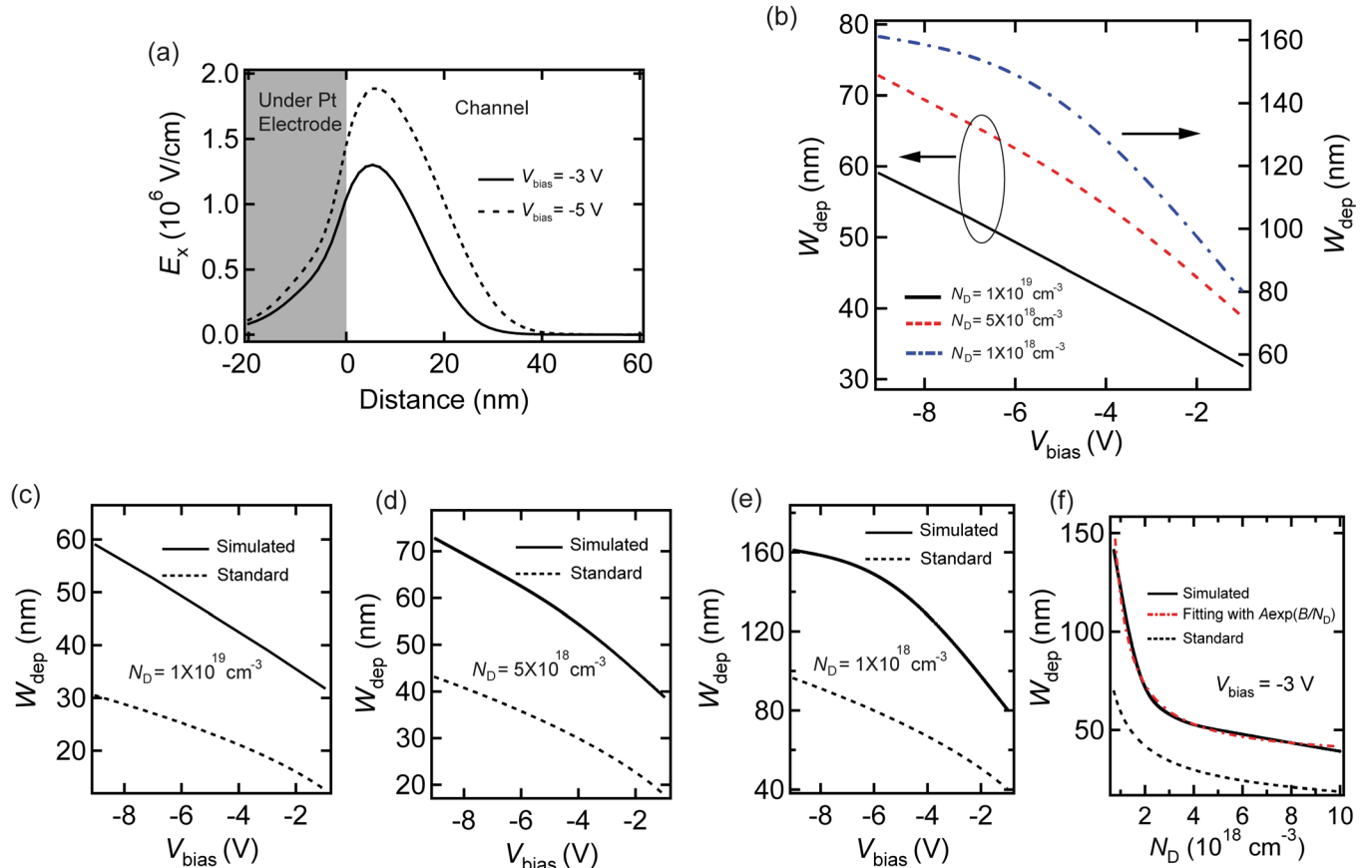


FIG. 3. (a) Spatial profiles of E_x taken from the middle of the nanowire for -3 V and -5 V biases; (b) simulated W_{dep} at different doping levels as a function of bias; (c)–(e) comparison of simulated W_{dep} and that calculated from standard bulk Schottky model as a function of bias at different doping levels; (f) comparison of simulated W_{dep} and that calculated from standard bulk Schottky model as a function of the doping level, with dotted-dashed red line as an exponential fitting.

Schottky diodes, and we address this with simulations of the current-voltage (I-V) relations. Particularly, we focus on the forward I-V characteristics, which are often used to extract fundamental parameters of Schottky junctions, including the ideality factor (which is unity for an ideal Schottky junction) and the barrier height. The simulated I-V curve (solid line), with N_D of $6.5 \times 10^{18} \text{ cm}^{-3}$, is plotted in Fig. 4(a). This agrees well with the experimental I-V curve (open circles) measured from a ZnO nanowire Schottky diode, suggests that the electrical transport process is well described by the simulations.

The ideality factor, η , and the barrier height, ϕ_B , are typically extracted through fitting the I-V curves using the procedures in Ref. 21. This commonly used analytical approach takes into account the series resistance (R) of a Schottky diode. Particularly, from the analytical thermionic emission model, the current is given by

$$I = A_d A^{**} T^2 \exp\left(-\frac{q\phi_B}{kT}\right) \times \exp\left[\frac{q(V_{\text{bias}} - IR)}{\eta kT}\right], \quad (3)$$

where A_d is the cross-section area of the diode, A^{**} is the Richardson constant, and R is the series resistance of the

Schottky diode. With the current density, J , given by I/A_d , we have

$$\frac{dV_{\text{bias}}}{d(\ln J)} = RA_d J + \frac{\eta}{\beta}, \quad (4)$$

where β is given by q/kT . The y-axis intercept of a plot of $\frac{dV_{\text{bias}}}{d(\ln J)}$ vs. J will yield $\frac{\eta}{\beta}$. ϕ_B can be obtained by defining a function $H(J)$

$$H(J) \stackrel{\text{def}}{=} V_{\text{bias}} - \frac{\eta}{\beta} \ln\left(\frac{J}{A^{**} T^2}\right). \quad (5)$$

From Eq. (3), we have

$$H(J) = RA_d J + \eta \phi_B. \quad (6)$$

Therefore, knowing η , the y-axis intercept of the plot of $H(J)$ vs. J yields ϕ_B . In practice, linear fittings to $\frac{dV_{\text{bias}}}{d(\ln J)}$ vs. J and $H(J)$ vs. J can be used to obtain the y-axis intercepts.

From the simulated I-V curve, the plots of $\frac{dV_{\text{bias}}}{d(\ln J)}$ and $H(J)$ are shown in Figs. 4(b) and 4(c), respectively. These plots show non-linear relations, different from those expected from Eqs. (4) and (6). Such a deviation from the linear relation has been observed from experimental studies of nanowire Schottky diodes.²² One possible origin of this non-linearity might be the electron velocity saturation effect, which is not considered in the analytical model. However, when excluding the electron velocity saturation, $\frac{dV_{\text{bias}}}{d(\ln J)}$ vs. J still shows the non-linear characteristic [inset to Fig. 4(b)], indicating that the different electrostatics in nanowire Schottky diodes plays the major role. This non-linearity prevents a reliable extraction of η and ϕ_B using the linear fitting. Therefore, the commonly used analytical approach is not suitable for analyzing nanowire Schottky diodes.

On the other hand, it can be instructive to estimate the ranges of η and ϕ_B , in the case that one nonetheless applies the analytical model. With linear fittings to different regions on the non-linear curve, as shown in Fig. 4(b) and its inset, η can be estimated to range from negative and less-than-unity values (which are unphysical) to the maximum value of 1.1, which is close to unity.²³ Therefore, the maximum value of η extracted using the analytical model might be used as an indication of the ideality of nanowire Schottky diodes. If η is taken to be at the value of 1.1, then $H(J)$ can be plotted according to Eq. (5), shown in Fig. 4(c), and the maximum value of ϕ_B can be estimated to be ~ 0.55 V from the linear fitting. We note that the Schottky barrier is defined to be 0.75 V for the simulations (Table I).¹⁵ The barrier lowering due to the image force was calculated to be ~ 0.11 V (not shown here), leading to an actual barrier height of ~ 0.64 V. Therefore, the analytical model underestimates ϕ_B . We note that lower-than-expected ϕ_B is often reported in nanowire Schottky diodes based on the analytical model, and is commonly taken as indications of non-ideal processes,^{22,24–26} including surface/interface states and defects, Fermi-level pinning, and carrier tunneling effects. Our findings suggest that the presence of these processes should not be claimed based on solely the low ϕ_B extracted from I-V curves using the analytical model.

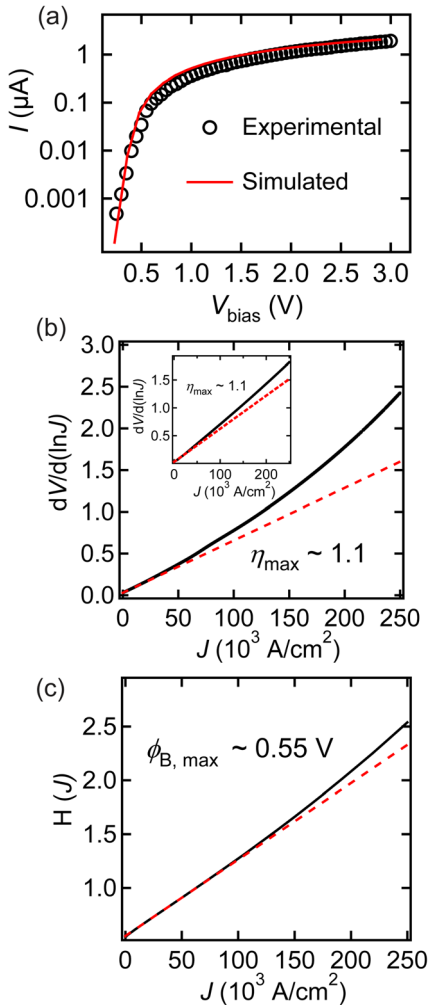


FIG. 4. (a) Simulated and measured forward-biased I-V curves of a nanowire Schottky diode; (b) plot of $dV/d(\ln J)$ vs. J , with the dashed line as the linear fitting that corresponds to the maximum value (1.1) of η , with the inset showing the same plot without the electron velocity saturation effect; (c) plots of $H(J)$ vs. J with $\eta = 1.1$, with the dashed line as the linear fitting that yield the maximum values (~ 0.55 V) of ϕ_B .

In summary, using 3D finite-element simulations, we have shown that, in semiconductor nanowire Schottky diodes, the standard and commonly used bulk model does not capture the electrostatics and electrical transport characteristics. Particularly, the depletion region width shows a linear (sublinear) dependence on the applied bias at high (low) doping levels, different from the square-root relation in the bulk model. The linear dependence agrees with previous experimental results. In all cases, the simulated depletion region width is significantly larger than that calculated using the bulk model. Additionally, simulations of the electrical properties, which agree well with experimental data, suggest that analyzing the current-voltage relations with the analytical thermionic emission model, as commonly done in previous studies, is in general not a valid approach to extracting important parameters, such as the ideality factor and the Schottky barrier height. To that end, numerical simulations should be used for evaluating nanowire Schottky diode performance and guiding nanowire device development efforts.

This work was supported by the National Science Foundation through the CAREER Program (DMR-0845007). We thank Afsoon Soudi for the ZnO nanowire growth.

- ¹U. Landman, R. N. Barnett, A. G. Scherbakov, and P. Avouris, *Phys. Rev. Lett.* **85**, 1958 (2000).
- ²F. Leonard and A. A. Talin, *Phys. Rev. Lett.* **97**, 026804 (2006).
- ³F. Leonard, A. A. Talin, B. S. Swartzentruber, and S. T. Picraux, *Phys. Rev. Lett.* **102**, 106805 (2009).
- ⁴J. S. Hwang, F. Donatini, J. Pernot, R. Thierry, P. Ferret, and L. S. Dang, *Nanotechnology* **22**, 475704 (2011).
- ⁵Y. Gu, E. S. Kwak, J. L. Lensch, J. E. Allen, T. W. Odom, and L. J. Lauhon, *Appl. Phys. Lett.* **87**, 043111 (2005).
- ⁶P. Y. Fan, U. K. Chettiar, L. Y. Cao, F. Afshinmanesh, N. Engheta, and M. L. Brongersma, *Nat. Photonics* **6**, 380 (2012).
- ⁷D. Martin, A. Heinzig, M. Grube, L. Geelhaar, T. Mikolajick, H. Riechert, and W. M. Weber, *Phys. Rev. Lett.* **107**, 216807 (2011).
- ⁸A. Soudi, P. Dhakal, and Y. Gu, *Appl. Phys. Lett.* **96**, 253115 (2010).
- ⁹J. E. Allen, E. R. Hemesath, D. E. Perea, J. L. Lensch-Falk, Z. Y. Li, F. Yin, M. H. Gass, P. Wang, A. L. Bleloch, R. E. Palmer, and L. J. Lauhon, *Nat. Nanotechnol.* **3**, 168 (2008).
- ¹⁰K. Sarpatwari, N. S. Dellas, O. O. Awadelkarim, and S. E. Mohny, *Solid-State Electron.* **54**, 689 (2010).
- ¹¹A. Soudi, E. H. Khan, J. T. Dickinson, and Y. Gu, *Nano Lett.* **9**, 1844 (2009).
- ¹²B. K. Meyer, H. Alves, D. M. Hofmann, W. Kriegseis, D. Forster, F. Bertram, J. Christen, A. Hoffmann, M. Strassburg, M. Dworzak, U. Haboeck, and A. V. Rodina, *Phys. Status Solidi B* **241**, 231 (2004).
- ¹³S. Kasap and P. Capper, *Springer Handbook of Electronic and Photonic Materials* (Springer, New York, 2006).
- ¹⁴P. C. Chang and J. G. Lu, *Appl. Phys. Lett.* **92**, 212113 (2008).
- ¹⁵S. M. Sze, *Physics of Semiconductor Devices*, 2nd ed. (Wiley, 1981).
- ¹⁶The diffusion theory model was not included because the effective electron diffusion velocity (v_D) is much larger than the effective recombination velocity (v_R); in fact, $v_D \sim 10 v_R$. In this case, the carrier transport across the Schottky barrier is dominated by the thermionic emission.
- ¹⁷C. Canali, G. Majni, R. Minder, and G. Ottaviani, *IEEE Trans. Electron Devices* **22**, 1045 (1975).
- ¹⁸See supplementary material at <http://dx.doi.org/10.1063/1.4765653> for details on the mobility model and the fitting.
- ¹⁹O. Hayden, G. F. Zheng, P. Agarwal, and C. M. Lieber, *Small* **3**, 2048 (2007).
- ²⁰F. Leonard and J. Tersoff, *Phys. Rev. Lett.* **83**, 5174 (1999).
- ²¹S. K. Cheung and N. W. Cheung, *Appl. Phys. Lett.* **49**, 85 (1986).
- ²²S. N. Das, J. H. Choi, J. P. Kar, K. J. Moon, T. Il Lee, and J. M. Myoung, *Appl. Phys. Lett.* **96**, 092111 (2010).
- ²³The slope of the linear fitting, according to Eq. (4), should be given by RA_d . This value can be estimated, in the case that the electron velocity saturation effect is excluded, to be $\sim 7.2 \times 10^{-10} \Omega \text{ m}^2$. However, the linear fitting with the slope of this value yields η to be ~ 0.25 , which is unphysical.
- ²⁴J. Kim, J. H. Yun, C. S. Han, Y. J. Cho, J. Park, and Y. C. Park, *Appl. Phys. Lett.* **95**, 143112 (2009).
- ²⁵A. Motayed, A. V. Davydov, M. D. Vaudin, I. Levin, J. Melngailis, and S. N. Mohammad, *J. Appl. Phys.* **100**, 024306 (2006).
- ²⁶W. F. Yang, S. J. Lee, G. C. Liang, R. Eswar, Z. Q. Sun, and D. L. Kwong, *IEEE Trans. Nanotechnol.* **7**, 728 (2008).